Influence of pore-scale disorder on viscous fingering during drainage

Renaud Toussaint,[1] Grunde Løvoll,[1] Yves Méheust,[2] Knut Jørgen Måløy,[1] and Jean Schmittbuhl[3]

[1] *Department of Physics, University of Oslo, POBox 1048 Blindern, N-0316 Oslo, Norway*
[2] *Department of Physics, NTNU Trondheim, N-7491 Trondheim, Norway*
[3] *Laboratoire de Géologie, École Normale Supérieure, 24 rue Lhomond, F-75231 Paris, France*

(Dated: February 2, 2008)

We study viscous fingering during drainage experiments in linear Hele-Shaw cells filled with a random porous medium. The central zone of the cell is found to be statistically more occupied than the average, and to have a lateral width of 40% of the system width, irrespectively of the capillary number Ca. A crossover length $w_f \propto Ca^{-1}$ separates lower scales where the invader's fractal dimension $D \simeq 1.83$ is identical to capillary fingering, and larger scales where the dimension is found to be $D \simeq 1.53$. The lateral width and the large scale dimension are lower than the results for Diffusion Limited Aggregation, but can be explained in terms of Dielectric Breakdown Model. Indeed, we show that when averaging over the quenched disorder in capillary thresholds, an effective law $v \propto (\nabla P)^2$ relates the average interface growth rate and the local pressure gradient.

PACS numbers: 47.20.Gv, 47.53.+n, 47.54.+r, 47.55.-t, 47.55.Mh, 68.05.-n, 68.05.Cf, 81.05.Rm.

Viscous fingering instabilities in immiscible two-fluid flows in porous materials have been intensely studied over the past 50 years [1], both because of their important role in oil recovery processes, and as a paradigm of simple pattern forming system. Their dynamics is controlled by the interplay between viscous, capillary and gravity forces. The ratio of viscous forces to the capillary ones at pore scale is quantified by the capillary number $Ca = \mu v_f a^2/(\gamma\kappa)$, where a is the characteristic pore size, v_f is the filtration velocity, γ the interfacial tension, κ the permeability of the cell, and μ the viscosity of the displaced fluid, supposed here much larger than the viscosity of the invading one.

There is a strong analogy between viscous fingering in porous media and Diffusion Limited Aggregation (DLA), as was first pointed out by Paterson [2]. Indeed, both processes of DLA and viscous fingering in empty Hele-Shaw cells belong to the family of Laplacian Growth Models, i.e. obey the Laplacian growth equation $\nabla^2 P = 0$, with an interfacial growth rate $v \propto -\nabla P$, where P is the diffusing field, i.e. the probability density of random walkers in DLA, or the pressure in viscous fingering. Despite differences as respectively a stochastic and deterministic growth, and boundary conditions as respectively $P = 0$ or $P = -\gamma/r$ with r the interfacial curvature, it is admitted that these processes belong to the same universality class [2, 3, 4]. In radial geometry these processes lead to fractal structures of dimensions $D = 1.70 \pm 0.03$ [5], 1.713 ± 0.0003 [6], and 1.7 [4] respectively in viscous fingering in empty Hele-Shaw cells, DLA, and numerical solutions of deterministic Laplacian growth. The two numerical models have been reexplored recently using stochastic conformal mapping theory [3, 4, 6]. However, in Hele-Shaw cells filled with disordered porous materials similar to the one used here, a lower fractal dimension $D = 1.58 \pm 0.09$ has been measured [7].

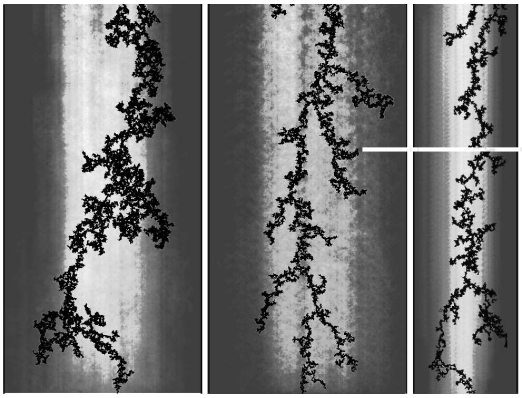

FIG. 1: *Invasion clusters on thresholded images at capillary numbers* Ca = 0.06 **(a)** *and* 0.22 **(b,c)**, *for* $W/a = 210$ **(a,b)***and* 110 **(c)**, *with displayed system lateral boundaries. The superimposed gray map shows the occupancy probability* $\pi(x, z)$ *of the invader, in a moving reference frame attached to the most advanced invasion tip and to the lateral boundaries.*

In straight channels, DLA gives rise to fractal structures of dimension 1.71, occupying on average a lateral fraction $\lambda = 0.62$ of the system width W [8]. Viscous fingering in empty Hele-Shaw cell converge towards the Saffman Taylor (ST) solution [9], with a uniformly propagating fingerlike interface covering a fraction $\lambda = 0.5$ of the system width at large capillary numbers [9, 10], selected by the interfacial tension [11].

In the system we study, the cell is filled with a disordered porous medium, and the non-wetting invader of low viscosity shows a branched structure that depends on Ca (Fig. 1). We will show theoretically that if indeed at high capillary number, the process is well described by DLA as often suggested [2], there is also at intermediate Ca a regime where the flow in *random* porous media is better described by another Laplacian model, namely a Dielectric Breakdown Model (DBM) with $\eta = 2$ – the interfacial growth rate is $v \propto (\nabla P)^\eta$ in DBM, $\eta = 1$ corresponding

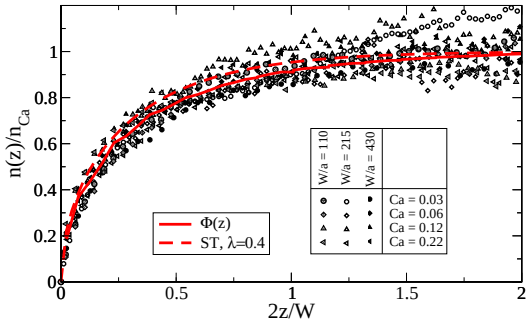

FIG. 2: *Scaled invader's density $n(z)/n_{Ca}$ as function of $2z/W$, distance to the most advanced tip scaled by the system's halfwidth, for three system sizes and four capillary numbers. The lines are the experimentally determined cumulative growth probability, and the theoretical Saffman Taylor solution for a single finger occupying a lateral fraction lambda = 0.4 of the system.*

to DLA –. Our conclusion is supported by both experimental evidence based on a characterization of the large- and small-scale geometry of the invader, and theoretical arguments based on averaging the capillary forces contribution to the interface growth rate over the pore scale randomness. The vanishing capillary number limit of our system corresponds to capillary fingering, where pores are invaded one by one, forming a propagating front filling the whole system, leaving behind isolated clusters of viscous fluid. The invader's fractal dimension is $D = 1.83$ [12], theoretically explained by the invasion percolation model [13]. At moderate but finite capillary numbers under interest here, we will show that small scales still correspond to invasion percolation, up to a crossover scale $w_f/a \propto Ca^{-1}$ characterizing the maximum size of isolated clusters of defending fluid, above which the system geometry can be described by the DBM with $\eta = 2$.

We study viscous fingering processes in linear Hele-Shaw cells of thickness $a = 1$mm filled at 38% with a monolayer of randomly located immobile glass beads of diameter a, between which air displaces a solution of 90% glycerol - 10% water of much larger viscosity $\mu = 0.165$ Pa·s, wetting the beads and walls of the cell, i.e. in drainage conditions. The interfacial tension and the permeability of the cell are respectively $\gamma = 0.064$ N·m^{-1} and $\kappa = 0.00166 \pm 0.00017$ mm^2. We investigate regimes ranging from capillary to viscous fingering ($0.01 < Ca < 0.5$), in cells with impermeable lateral walls and dimensions $W \times L \times a$, with widths perpendicularly to the flow direction $W/a = 110$, 215 and 430, and a length $L/a = 840$. The cell is set horizontally, so that gravity is irrelevant. A constant filtration rate of water-glycerol is ensured by a controlled gravity-driven pump.

Pictures of the flow pattern are taken from the top, and treated to extract the invading air cluster (with pixels of size $0.55a$), as the black clusters in Fig. 1. In ref. [14], we have shown that the invasion process is stationary, up to fluctuations arising from the disorder in pore geometries. To extract the underlying average stationary behavior, all quantities are then analyzed in the reference frame (x, z) attached to the lateral boundaries at $x = 0$ and $x = W$, and to the foremost propagating tip at $z = 0$, z pointing against the flow direction (this tip indeed propagates at a roughly constant speed v_{tip} [14]). Average quantities at any position (x, z) of the tip related frame, are defined using all stages and points of the invasion process, excluding regions closer than $W/2$ from the inlet or outlet, to avoid finite size effects.

The average occupancy map $\pi(x, z)$ is defined as [14]: for each time (or each picture), we assign the value 1 to the coordinate (x, z) if air is present there, 0 otherwise. $\pi(x, z)$ obtained as the time average of such occupancy function, is displayed as graymap in Fig. 1.

Next we compute the average number of occupied pores per unit length at a distance z behind the tip, $n(z)$, which is related to π as $n(z) = (1/a^2) \int_0^W \pi(x, z)\, dx$. We show in Fig. 2 a data collapse for different capillary numbers Ca and system widths W, $n(z)/n_{Ca} = \Phi(2z/W)$, where $n_{Ca} = (W/a^2)v_f/v_{tip}$ [14]. Φ is a function increasing from 0 at $z = 0$ towards 1 at $z = +\infty$, as granted by conservation of the displaced fluid for a statistically stationary process [14]. Φ evaluated in Fig. 2 is a cumulative growth probability defined in Ref. [14], and is obtained as an average over all experiments and sizes.

We also characterize the lateral structure of the invader in the frozen zone, $z > W$, where less than 10% of the invasion activity takes place since $\Phi(2) > 0.9$. We define over this zone a distribution $\rho(x) = [W/(a^2\, n_{Ca})]\ \pi(x, \infty) = (v_{\rm tip}/v_{\rm f})\ \pi(x, \infty)$, so that $\int_0^W \rho(x)dx/W \simeq 1$. This quantity, presented in Fig. 3(a) for an average over five experiments at capillary numbers $Ca = 0.06$ and 0.22 for $W/a = 215$, and over four experiments with $0.06 < Ca < 0.22$ for $W/a = 110$, is reasonably independent of the capillary number and the system size, though the noise is larger at highest speed. The fraction λ of the system, occupied by the invader at saturation is evaluated as in [8]: $\lambda = 1/\rho_{max}$, or alternatively $\lambda = (x^+ - x^-)/W$, where $\rho(x^+) = \rho(x^-) = \rho_{max}/2$. Both definitions lead to $\lambda \simeq 0.4 \pm 0.02$ for the capillary numbers probed, as shown in Fig. 3(a), which is significantly smaller than the off-lattice DLA result $\lambda = 0.62$ [8, 15].

The 2D occupancy map $\pi(x, z)$ itself, displayed as graymap in Fig. 1, has a maximum $\pi_{\rm max} = \rho_{\rm max} v_f/v_{\rm tip}$, along a line at $(x = W/2, z > W)$. Similarly to Arneodo's procedure [8], we determine the support of $\pi > \pi_{max}/2$, displayed in Fig. 3(b) and (c), which corresponds to the most often occupied region. Within the noise error, the shape of this region resembles the theoretical ST curve corresponding to this $\lambda = 0.4$ [9] (gray lines in Fig. 3). For such ST finger, this curve would also correspond to

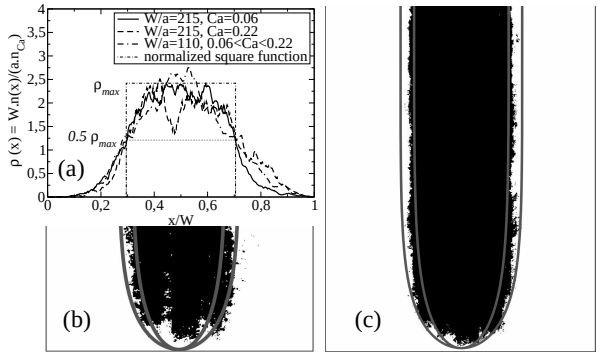

FIG. 3: *(a) Normalized occupation density $\rho(x)$, with half-maximum reached over a width $0.4W$. (b,c) Average occupation density map of the invader thresholded at half-maximum, for a system size W/a=215, in the reference frame attached to the tip position, at $Ca = 0.06$ (b) and 0.22 (c), compared to ST curves for $\lambda = 0.35$ and 0.45.*

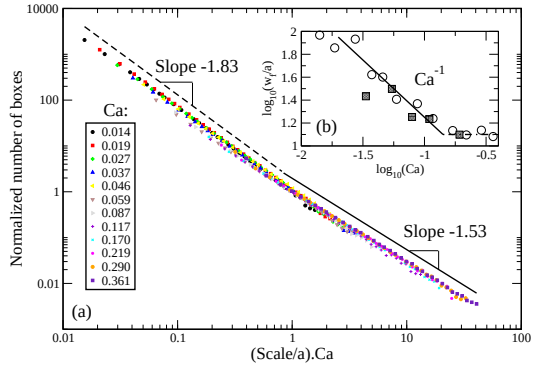

FIG. 4: *(a) Mass fractal dimension of the invasion cluster at various capillary numbers. (b): Cross-over scale w_f between capillary and viscous scales, as function of Ca.*

the scaled longitudinal density of invader $\Phi(z)$. $\Phi(z)$ determined for our experiments (continuous line in Fig. 2) and this theoretical ST shape (dashed line) also present some similarities. Systematic deviations from the mathematical ST solution at $\lambda = 0.4$ might nonetheless exist, since they have been seen between the DLA envelopes and the corresponding ST solution at $\lambda = 0.62$ [15].

The mass fractal dimension of the invasion clusters is analysed by box-counting. $N(s)$ is the number of boxes of size s to cover the invader. Fig. 4 displays a normalized distribution $N(s)/N(a/Ca)$ as function of $(s/a) \cdot Ca$ for various capillary numbers. By linear regression of this collapsed log-log data, we find that $N(s) \sim s^{-1.83\pm0.01}$ for small scales $s < a/Ca$, and $N(s) \sim s^{-1.53\pm0.02}$ for larger scales. The result can be explained by the following approximations. The distribution of pore throats sizes results in a distribution of capillary pressure thresholds P_t, $g(P_t)$, of characteristic width W_t. Consider a box of size w_f along the cluster boundary in the active zone, such that $w_f \cdot \nabla P_b = W_t$ where ∇P_b is a characteristic pressure gradient. At scales $s < w_f$, viscous pressure variations are lower than capillary threshold fluctuations, and the most likely invaded pores correspond to the lowest random thresholds, which corresponds to capillary fingering, thus leading to $D = 1.83$. Conversely, at larger sizes ($s > w_f$), the invasion activity is determined essentially by the spatial variations of ∇P_b. Assuming that ∇P_b scales as the imposed $\nabla P(-\infty) \propto Ca$, i.e. neglecting the geometry variations between different speeds, w_f scales as $W_t/\nabla P_b \propto a/Ca$, as confirmed by the data collapse in Fig. 4(a). w_f can also be determined experimentally as a characteristic branch width, since capillary fingering leaves isolated clusters of trapped fluid, whereas the large scale structure is branched. After removing all trapped clusters, we determine w_f as the average length of intersects of the structure from cuts along x. Indeed, Fig. 4(b) is consistent with a scaling law $w_f/a \propto Ca^{-1}$, below a saturation at large Ca.

Eventually, we sketch a possible explanation for the width selection $\lambda = 0.4$ and the large scale fractal dimension $D = 1.53 \pm 0.02$, which are smaller than their counterparts in DLA, respectively 0.62 and 1.71. Neglecting the small scale permeability variations leads to a Laplacian pressure field in the defending fluid. The boundary condition for the pressure field is then $\nabla P(z = -\infty) = -\mu v_f/\kappa$, and $\nabla P(x = 0, W) \cdot \hat{x} = 0$ where $\hat{x}$ is the unit vector along x. The dynamics of the process is then entirely controlled by the boundary condition along the invading fluid, i.e. by the capillary pressure drop across the meniscus in the pore neck and the pressure gradient in the invaded fluid. For a given pressure difference at pore scale between the invading air at P_0, and the pressure P_1 in the glycerol-filled pore, we decompose $P_0 - P_1 = \Delta P_v + P_c$, where ΔP_v is a viscous pressure drop in the pore neck, and the capillary pressure drop is $P_c = \gamma/r + 2\gamma/a$, where the in- and out-of-plane curvature of the interface are respectively r and $a/2$. As a meniscus progresses between neighboring beads, its curvature goes through a minimum r_m in the pore neck. The meniscus will be able to pass the neck if the pressure drop $P_0 - P_1$ exceeds the threshold $P_t = P_c(r_m)$. For the sake of simplicity, the probability distribution of the thresholds $g(P_t)$ is considered flat, between P_{min} and P_{max}, with $W_t = P_{max} - P_{min}$ and $g(P_t) = \theta(P_t - P_{min})\theta(P_{max} - P_t)/W_t$, where θ is the Heaviside function. In the pure capillary fingering limit $Ca \to 0$, the pressure field P is homogeneous in the defending fluid, and a pore is invaded when $P_0 - P$ reaches the minimum threshold along the boundary, close to P_{min}. At higher capillary number, we want to relate the invasion rate to the local capillary threshold, and to the pressure P_1 in the liquid-filled pore nearest to the interface. If $P_0 - P_1 < P_t$, the meniscus adjusts reversibly in the pore neck, and the next pore is not invaded. Conversely, if $P_0 - P_1 > P_t$, the pore will be invaded, and most of the invasion time is spent in the thinnest region of the pore neck. A characteristic interface velocity can

be evaluated by the Washburn equation [16] at this point: $v \sim -(2\kappa/\mu a)(P_0 - P_1 - P_t)\theta(P_0 - P_1 - P_t)$, where the heaviside function results from a zero invasion velocity if the pore is not invaded. Hypothesizing that only the average growth rate controls the process, independently of the particular realization of random thresholds, the growth rate averaged over all possible pore neck configurations, is

$$\begin{aligned} < v > &= \int \frac{-2\kappa}{\mu a}(P_0 - P_1 - P_t)\theta(P_0 - P_1 - P_t)g(P_t)dP_t \\ &= -(\kappa/\mu a)\theta(P_0 - P_1 - P_{min}) \times \\ &\quad \{[(P_0 - P_1 - P_{min})^2/W_t]\theta[P_{max} - (P_0 - P_1)] + \\ &\quad 2[P_0 - P_1 - (P_{min} + P_{max})/2]\theta[P_0 - P_1 - P_{max}]\}. \end{aligned} \quad (1)$$

At moderate capillary numbers, such as $P_0 - P_1 < P_{max}$, if we assume that the capillary pressure drop is around $P_c = P_{min}$ when the invasion meniscus is at the entrance of the pore neck, we note that $(P_0 - P_{min} - P_1)/a = \Delta P_v/a \sim \nabla P/2$, and Eq. (1) implies that the growth rate goes as $< v >= -a\kappa/(4\mu W_t)(\nabla P)^2$. This effective quadratic relationship between the average growth rate and the local pressure gradient arises from the distribution of capillary thresholds, and means that such invasion process should be in the universality class of DBM with $\eta = 2$, rather than DLA (DBM, $\eta = 1$). Indeed, in DBM simulations in linear channels, λ is a decreasing function of η (as in related deterministic problems, as viscous fingering in shear-thinning fluids [17], or η-model [18]), and Somfai et al. [15] report $\lambda \simeq 0.62$ and 0.5 for respectively $\eta = 1$ and 1.5, so that the observed $\lambda = 0.4$ is consistent with $\eta = 2$. The fractal dimension of DBM is also a decreasing function of η, and $\eta = 2$ corresponds $D = 1.4 \pm 0.1$ [19], which is close to the observed $D = 1.53 \pm 0.02$ in our experiments.

Note that at high capillary numbers such that locally $P_0 - P_1 \gg P_{max}$, the threshold fluctuations are not felt by the interface, and Eq. (1) leads to $< v_{inv} >= -(\kappa/\mu)\nabla P$, which would correspond to a classic DLA process. We have checked by numerically solving the Laplace equation with the experimental clusters as boundaries that all experiments performed here were at moderate enough capillary number to have $P_0 - P_1 < P_{max}$ all along the boundary [14], i.e. the quadratic law $< v >= -a\kappa/(4\mu W_t)(\nabla P)^2$ is expected to hold.

Even at moderate Ca, deviations from the DBM model with $\eta = 2$ could be observed for significantly non-flat distribution of the capillary thresholds in the random porous medium, for which Eq.(1) would lead to a more complicated dependence of the growth rate v on ∇P, reflecting the details of this distribution, and not simply a power-law effective relationship. It would be interesting in future work to explore numerically and experimentally the detailed effect of non-flat capillary threshold distributions on the selected fractal dimension, average width occupied in the system, and total displaced mass $n_{Ca}(Ca)$ (reported in [14] for the present work), to extract the influence of the disorder on the best capillary number to select in order to maximize the efficiency of the extraction process.

We acknowledge with pleasure fruitful discussions with E. G. Flekkøy, A. Lindner, A. Hansen and E. Somfai. This work was supported by the CNRS/NFR PICS program, and the NFR Petromax program.

[1] D. Bensimon, L. P. Kadanoff, S. Liang, B. I. Shraiman, and C. Tang, Rev. Mod. Phys. **58**, 977 (1986).
[2] L. Paterson, Phys. Rev. Lett. **52**, 1621 (1984).
[3] M. G. Stepanov and L. S. Levitov, Phys. Rev. E **63**, 061102 (2001).
[4] A. Levermann and I. Procaccia, Phys. Rev. E **69**, 031401 (2004).
[5] E. Sharon, M. G. Moore, W. D. McCormick, and H. L. Swinney, Phys. Rev. Lett. **91**, 205504 (2003).
[6] B. Davidovitch, A. Levermann, and I. Procaccia, Phys. Rev. E **62**, R5919 (2000).
[7] E. L. Hinrichsen, K. J. Måløy, J. Feder, and T. Jøssang, J. Phys. A **22**, L271 (1989); K. J. Måløy, J. Feder, and T. Jøssang, Physical Review Letters **55**, 2688 (1985).
[8] A. Arneodo, J. Elezgaray, M. Tabard, and F. Tallet, Phys. Rev. E **53**, 6200 (1996).
[9] P. G. Saffman and G. Taylor, Proc. Soc. London **Ser. A 245**, 312 (1958).
[10] P. Tabeling, G. Zocchi, and A. Libchaber, J. Fluid Mech. **177**, 67 (1987).
[11] J. W. McLean and P. G. Saffman, J. Fluid Mech. **102**, 445 (1981); B. I. Shraiman, Phys. Rev. Lett. **56**, 2028 (1986).
[12] R. Lenormand and C. Zarcone, Physical Review Letters **54**, 2226 (1985).
[13] R. Chandler, J. Koplik, K. Lerman, and J. F. Willemsen, Journal Fluid Mechanics **119**, 249 (1982).
[14] G. Løvoll, Y. Méheust, R. Toussaint, J. Schmittbuhl, and K. J. Måløy, Phys. Rev. E **70**, 026301 (2004).
[15] E. Somfai, R. C. Ball, J. P. DeVita, and L. M. Sander, Phys. Rev. E **68**, 020401(R) (2003).
[16] E. W. Washburn, Phys. Rev. **17**, 273 (1921).
[17] A. Lindner, D. Bonn, E. Corvera Poiré, M. Ben Amar, and J. Meunier, J. Fluid Mech. **469**, 237 (2002).
[18] M. Ben Amar, Phys. Rev. E **51**, R3819 (1995).
[19] J. Mathiesen and M. H. Jensen, Phys. Rev. Lett. **88**, 235505 (2002); E. Somfai et al. (2004), cond-mat/0401384; L. Pietronero and E. Tossati, eds., *Fractals in Physics* (North-Holland, 1986), p. 151.